Unintentional doping of a-plane GaN by insertion of in situ SiN masks

H Witte, M Wieneke, A Rohrbeck, K -M Guenther, A Dadgar, A Krost

Unintentional Doping of a-Plane GaN by Insertion of In-situ SiN-masks

H Witte, M Wieneke, A Rohrbeck, K –M Guenther, A Dadgar and A Krost

Institute of Experimental Physics, Otto-von-Guericke-Universitity-Magdeburg, MB 4120, 39016 Magdeburg, Germany

E-mail: hartmut Witte@physik.uni-magdeburg.de

Abstract

Undoped a-plane GaN layers grown by metal organic vapor phase epitaxy on sapphire (10-12) substrates using low temperature GaN seed layers and in-situ SiN masks were characterized by Hall-effect measurements, CV-characteristics and photovoltage spectroscopy. With increasing deposition time of the SiN masks the electron concentrations of the GaN layers are enhanced. The dominant activation energy between 14 meV and 22 meV determined by temperature dependent Hall-effect is very similar to the donor silicon on gallium site. Two other activation energies at 30 meV and between 50 meV and 70 meV were found corresponding well with O_{Ga} and V_N defects, respectively. The depth profiles of the net donor densities show a strong increase towards the substrate /LT-GaN/HT-GaN interface indicating diffusion of silicon from the SiN mask towards the surface. Therefore, the Si-doping is attributed to the dissolution of the SiN masks during the following high temperature GaN layer growth. Si-doping from the SiN masks also explains the deterioration of the band bending within the LT-GaN / HT-GaN junction found by photovoltage spectroscopy.

1. Introduction

GaN-based materials are used in optoelectronic and microelectronic devices like LEDs, vertical cavity surface emitting lasers or high electron mobility transistors. In some applications strong piezoelectric fields in c-plane GaN based multilayer are undesired evoking for instance the quantum confined stark effect (QCSE). In this case the reduced polarization field of non c-plane GaN layers is useful for an enhanced radiative recombination rate [1]. Unfortunately, due to its anisotropic nature hetero-epitaxial growth of non-polar GaN produces much more stacking faults than c-axis oriented GaN. The basal and prismatic plane stacking faults act as defects, which are well known from photoluminescence measurements [2].

The high density of stacking faults can be reduced by using an in-situ SiN nano mask described in detail by [3], [4], [5], and [6]. Otherwise, Si-doping of a-plane GaN increases the density of screw dislocations and decreases the density of edge dislocations resulting in an increase of the mobility [7]. Therefore, we have to proof if the reduction of stacking faults is introduced directly by the SiNx-mask or by the unintentionally Si-doping of the GaN layers due to these nano masks.

We have investigated the electrical properties of unintentionally doped a-plane GaN layers with in-situ SiN masks in dependence on the deposition time of the SiN layer. A strong doping effect due to the SiN masks was found combined with a doping gradient towards the substrate / SiN mask interface.

2. Experimental Details

All samples investigated here were grown by metal-organic vapor phase epitaxy on (10-12) sapphire substrates using a low temperature (LT) GaN seed layer with a thickness of 65 nm grown at 540 ^{0}C. A series of samples with varying growth times of the SiN-mask between 0 and 240 s deposited in the LT-GaN / GaN interface at 1145 ^{0}C was investigated (fur-

ther details in Ref. 6). Under these conditions, a non closed SiN insertion layer acting as an in-situ mask is formed. Therefore, the Si concentration in these mask regions cannot be estimated. On top GaN was grown at 1145 ^{0}C with a thickness of 2.5 µm to 3 µm. These masks produce areas of significantly reduced densities of crystallographic defects accompanied by arrow like pits in c-plane direction [6].

The carrier concentrations and mobilities were determined by conductivity and Hall-effect measurement in van der Pauw contact geometry with four Indium dots as Ohmic contacts. A constant measurement current of 1 mA and a magnetic induction of 330 mT were used. The measurement temperature was varied between 100 K and 400 K using a liquid nitrogen cryostat. For the CV-characteristics at room temperature mercury contacts with small and large areas were used as Schottky and Ohmic contacts, respectively, in coplanar contact arrangement. From the slope of $1/C^2$ versus V the net donor concentrations (N_D-N_A, with N_D and N_A the donor and acceptor concentration) were determined which are equal to the electron concentration in the case of fully ionized donor states.

PV measurements were taken with a dual-phase lock-in amplifier at 0V bias voltage and a chopper frequency of 63 Hz. At wavelengths ranging from 200 to 900 nm the illumination was realized with a xenon lamp and a grating monochromator, and between 600 and 1100 nm with a mercury lamp/grating monochromator arrangement. All measurements were done under the same experimental conditions such as xenon lamp power, a slit width of 1 mm, the same monochromator and a uniform excitation spot on the sample with a size of (3*8)mm^2. The circular Ohmic contacts with a diameter of 0.75 mm consisted of Indium dots which were heated up to 350 $^\circ$C. The two contacts used in these measurements are arranged on top of the samples with a distance of 5mm to avoid any illumination of the contact area.

3. Results and Discussion

Unintentionally doped GaN layers show both an increased conductivity and an increased electron concentration with enhanced deposition times of the SiN mask as shown in figure 1. For non-intentionally Si- doped layers the sheet conductivities and the sheet electron densities are given. Implying a homogeneous distribution of the donor levels in the GaN layers with a thickness of about 3 µm the resulting carrier concentration and conductivity varied between $6*10^{17}$ cm^{-3} and $2.1*10^{18}$ cm^{-3} ,and between 0.06 and 1.3 $(\Omega cm)^{-1}$, respectively.

Furthermore, at short deposition times the measured Hall mobility increases and decreases at longer deposition times (see figure 2) showing a broad maximum exceeding 50 cm^2/Vs at about 100 s which is similar to the Si-doping dependent mobility of a-plane GaN [7]. At lower deposition times the increased mobility can be explained by the increased crystallographic quality deduced from the decrease of the ω FWHM of the in-plane GaN Bragg reflections shown for the same samples in [8]. At higher SiNx deposition times not only the Si-doping level increases but also the surface morphology shows pits with increasing density and size [8]. Therefore, the decreasing mobilities can be caused by the formation of a Silicon impurity band (degradation) and/or by the morphological disturbances.

Investigations of undoped a-plane GaN layers without a SiN mask grown under similar conditions yields high resistance layers with a specific resistivity more than 10^6 Ωcm [9]. Thus, the doping effect in the samples with SiN masks can only be explained by the dissolution of the SiN mask during the subsequent growth process of the a-plane GaN layer.
Therefore, we measured the temperature dependent Hall coefficient (TDH) of some samples of this series and determined the thermal activation energies from the $\ln(R_H T^{3/2})$-1/T-slope shown in figure 3 and summarized in table 1.

For the interpretation of these results it should be noted that the samples include a doping profile with a near interface region which is strongly Si doped by the SiNx masks and a near surface region with a low Si doping level. Because the Hall-effect signals always stem from the most conductive layer, the measured electron concentrations involve mainly the near

interface region in our samples. Caused by the high doping level in this region the temperature dependent Hall coefficient may be controlled by an impurity level band characterized by a low temperature dependence of the Hall coefficient. Nevertheless, samples grown with SiN masks show activation energies only from 16 meV to 20 meV in the range between 95 K and 160 K which is well known for the shallow Si donor [10].

At higher temperatures further donor levels with higher activation energies are ionized increasing the conductivity of the lower Si doped regions. Therefore, the temperature dependent Hall coefficient increases and reaches a second activation energy at 30 meV in the intermediate temperature range and finally values up to 64 meV. These measured activation energies represent the sum of all thermal ionization energies of the existing donors. For instant, the activation energies of silicon on Ga site and oxygen on nitrogen site in c-plane GaN are 22 meV and 34 meV, respectively [10], [11]. In addition, a high temperature donor level at about 60 meV is attributed to an intrinsic defect. As shown in [10] the nitrogen vacancy has an activation energy of 64 meV which is within the measurement error of our values for the samples with deposition times below 100 s.

For higher deposition times the activation energies in the low temperature region are very low between 14 meV and 16 meV. For these samples the corresponding plots in figure 3 show no clearly separated high temperature slopes. Therefore, these activation energies are probably be caused by the high concentration of the shallow Si donor. These lower values of thermal activation energies are further indications of screening and degeneracy effects at higher silicon concentrations [11].

In conclusion, our samples are unintentionally Si-doped by using the SiN mask deposited onto the GaN buffer layer. Under these conditions we expect a decrease of the donor concentration from the SiN-mask towards the sample surface. This assumption was proofed by CV-characteristics. As shown in figure 4, with increasing bias voltage the net donor concentrations increase. In coplanar contact arrangement zero biasing is sensitive to the near surface

region and higher biasing to the interface region. This behavior is in good agreement with our assumption of the SiN mask as the doping source and the diffusion of the Si atoms from the SiN mask into the growing GaN layer creating a doping profile.

Next to the surface the net donor concentrations are in the range of (0.2- 1.5) $*10^{16}$ cm^{-3} and increase up to (1.0-2.0) $*10^{16}$ cm^{-3} towards the SiN mask. These donor concentrations are very low compared to the volume electron concentrations from the Hall-effect measurements (more than $6*10^{17}$ cm^{-3}). This discrepancy is caused by the fact that the Hall-effect measurements determine the carrier concentrations within the most conducting region which is represented by the SiN-mask/GaN interface.

In samples with a SiN-mask also Photovoltage spectroscopy reveals a different behavior. The measured open-circuit voltage depends on internal electric fields in pn-junctions or heterostructures and is controlled by the generation and recombination of light induced carriers within the whole samples and by the carrier diffusion towards the junction regions [12]. All undoped a-plane GaN layers without a SiN-mask and the one with the lowest SiN deposition time show band gap absorption edge of GaN and a peak between 369 nm and 372 nm.
The effect can be explained by assuming a band bending at the LT-GaN/HT-GaN interface in the case of undoped samples. In samples with SiN masks the band bending is released by Si doping of both the LT-GaN and the HT-GaN layer resulting in non-measurable photovoltages.

4. Summary

The electrical properties of a-plane GaN layers containing SiN masks were characterized by conductivity and Hall-effect measurements, CV-characteristics, and photovoltage spectroscopy. With increasing deposition times of the SiN masks the conductivity and the electron concentrations increase suggesting the thickness of the SiN mask to be responsible. From temperature dependent Hall-effect silicon on gallium site is the most probable dominat-

ing donor with an activation energy at about 22 meV. Two other activation energies at 30 meV and between 50 meV -70 meV correspond well to O_{Ga} and V_N defects known in c-plane GaN.

The net donor concentrations in these samples are in the range of some of 10^{16} cm^{-3} determined by CV-characteristics and more than one order of magnitude higher in Hall-effect measurements. Therefore, the doping level must be inhomogeneous within the GaN layer. The depth profiles of the net donor densities show a strong increase from the surface towards the substrate. All findings can be satisfactory explained by the SiN masks as a source of Si-doping.

Acknowledgment

The authors gratefully acknowledge support from Deutsche Forschungsgemeinschaft in the framework of the Research Unit 957.

References

[1] Waltereit P, Brandt O, Trampert A, Grahn HT, Menniger J, Ramsteiner M, Reiche M, and Ploog KH 2000 NATURE **406** 865

[2] BastekB, August O, Hempel T, Christen J, Wieneke M, Bläsing J, Dadgar A, Krost A, and Wendt U 2010 Appl. Phys. Lett. **96** 172102

[3] Chakraborty A, Kim KC, Wu F, Speck JS, DenBaars SP, and Mishra UK 2006 Appl. Phys. Lett. **89** 041903

[4] Johnston CF, Kappers MJ, Moram MA, Hollander JL, Humphreys CJ 2009 J. Cryst. Growth **311** 3295

[5] Ko S, Wang TC, Huang HM, Chen JR, Chen HG, Chu CP, Lu TC,. Kuo HC, and Wang SC 2008 J. Cryst. Growth **310** 4972

[6] Wieneke M, Bläsing J, Dadgar A, Veit P, Metzner S, Bertram F, Christen J, and Krost A 2009 Phys. Stat. Sol. C **6** 5498

[7] Ma B, Miyagawa R, Hu W, Li DB, Miyake H, and Hiramatsu K 2009 J. Cryst. Growth **311** 2899

[8] Wieneke M, Noltemeyer M, Bastek B, Rohrbeck A, Witte H, Veit P, Blaesing J, Dadgar A, Christen J, Krost A 2010 Phys. Stat. Sol. B DOI 10.1002 / pssb.201046372

[9] Witte H, Guenther KM, Wieneke M, Blaesing J, Dadgar A, and Krost A 2009 Physica B **404** 4922

[10] Look DC, Reynolds DC, Hemsky JW, Sizelove JR, Jones RL, and Molnar RJ 1997 Phys. Rev. Lett. **79** 2273

[11] Goetz W, Johnson NM, Chen C, Liu H, Kuo C , and Imler W 1996 Appl. Phys. Lett., **88** 3144

[12] Witte H, Hums C, Baer C, Guenther KM, Krtschil A, Dadgar A and Krost A 2009 .J Phys. D: Applied Physics **42** 205103

Figure Captions

Figure 1. Sheet electron concentration n_s and sheet conductivity σ_S at 295 K versus the deposition time of the SiN mask. Samples grown without SiN mask show sheet conductivities below $5*10^{-7}$ $(m\Omega)^{-1}$.

Figure 2. Hall mobility at 295 K versus the deposition time of the SiN mask.

Figure 3. Arrhenius plots of the Hall coefficient for determination of the activation energies. The samples with thinner SiN layers (lower deposition times) show up to three different slopes summarized in table 1.

Figure 4. Net donor concentration profiles determined by CV-characteristics at 50 kHz for the samples shown in figure 3. The donor concentration increases from the surface towards the substrate.

Figure 5. Open circuit photovoltage spectra of different samples. Only the sample without and with the thinnest SiN layers show a GaN band-band-generation at 358 nm and a defect related signal at about 370 nm. These features are not observed in samples with thicker SiN layers.

Table 1: Thermal activation energies E_A determined from the $\ln(R_H T^{3/2})$-1/T-slope shown in figure 3.

Deposition Time (s)	E_A (meV) 95K-160K	E_A (meV) 200K-250K	E_A (meV) 300K-400K
15	16±1		55.8±0.4
30	20±2	30.6±3	60.2±0.8
140	16±1		45.2±0.2
200	14±0.5		41±2

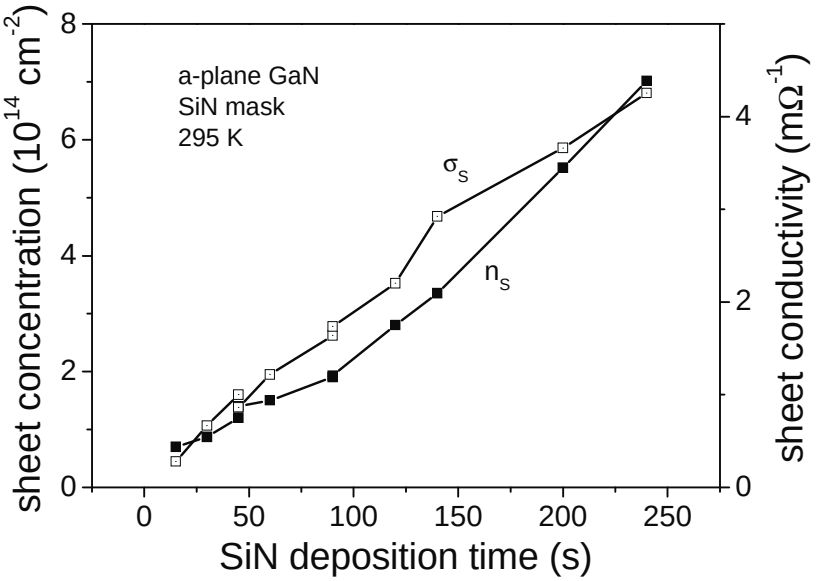
a-plane GaN
SiN mask
295 K
σS
nS
sheet concentration (10^14 cm^-2)
sheet conductivity (mΩ^-1)
SiN deposition time (s)
0
2
4
6
8
0
50
100
150
200
250

Figure 1

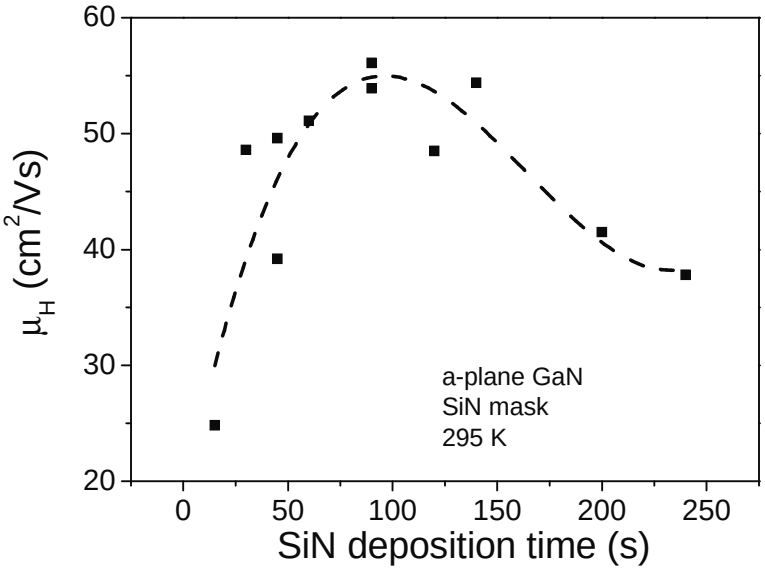
60
50
40
30
20
0
50
100
150
200
250
μ_H (cm^2/Vs)
SiN deposition time (s)
a-plane GaN
SiN mask
295 K

Figure 2

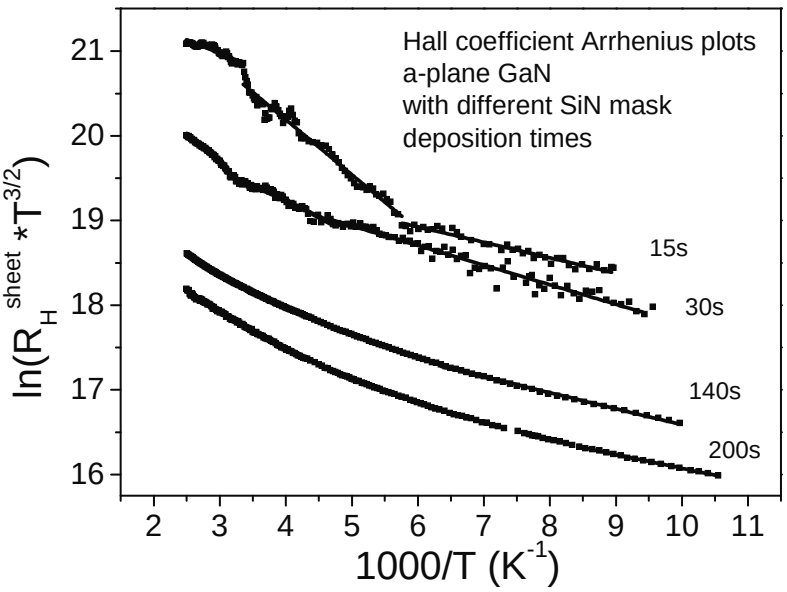
Hall coefficient Arrhenius plots
a-plane GaN
with different SiN mask
deposition times
15s
30s
140s
200s
ln(R_H^sheet *T^3/2)
1000/T (K^-1)
21
20
19
18
17
16
2
3
4
5
6
7
8
9
10
11

Figure 3

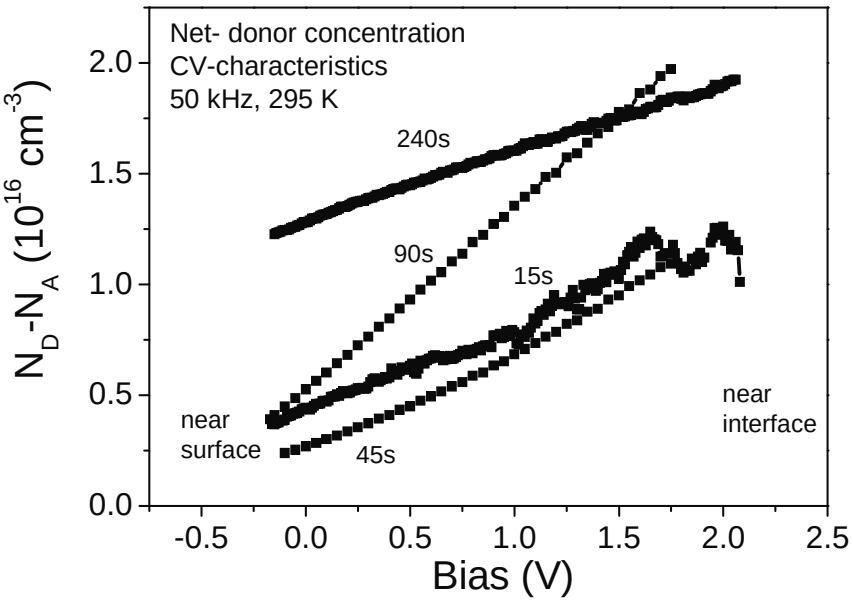
Net- donor concentration
CV-characteristics
50 kHz, 295 K
240s
90s
15s
45s
near
surface
near
interface
N_D-N_A (10^{16} cm^{-3})
Bias (V)
2.0
1.5
1.0
0.5
0.0
-0.5
0.0
0.5
1.0
1.5
2.0
2.5

Figure 4

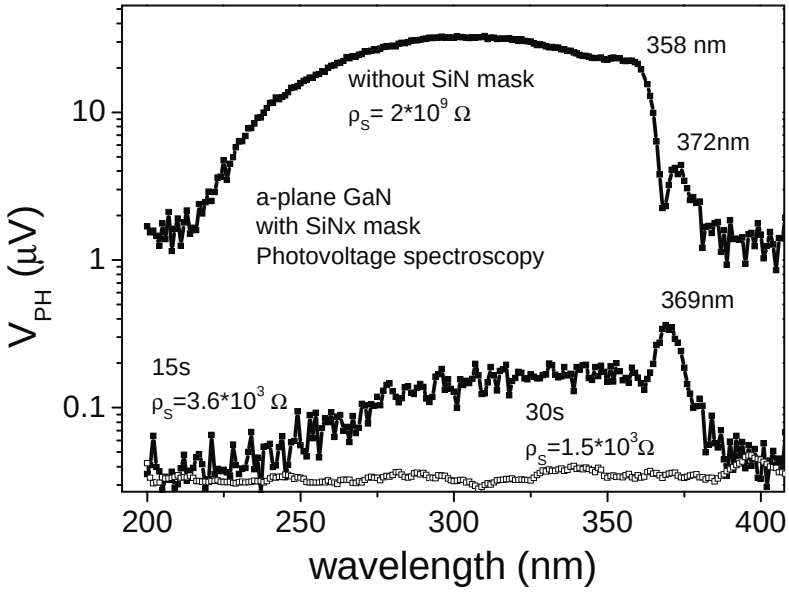
358 nm
without SiN mask
ρ_S= 2*10^9 Ω
372nm
a-plane GaN
with SiNx mask
Photovoltage spectroscopy
369nm
15s
ρ_S=3.6*10^3 Ω
30s
ρ_S=1.5*10^{3}Ω
10
1
0.1
V_{PH} (μV)
200
250
300
350
400
wavelength (nm)

Figure 5